Structure and Fragmentation Mechanisms of Isomeric T-Rich Oligodeoxynucleotides: A Comparison of Four Tandem Mass Spectrometric Methods

Z. Wang, Katty X. Wan, R. Ramanathan, John S. Taylor, and Michael L. Gross
Department of Chemistry, Washington University, St. Louis, Missouri, USA

Understanding the product-ion spectra of T-rich tetradeoxynucleotides is a starting point in the development of a mass spectrometric scheme to determine the mutagenicity of individual types of DNA damage. We obtained product-ion spectra for electrospray-produced ions that were activated in the ion source (electrospray ionization-source collision-activated-dissociation) and by high-energy collisions in the MS/MS mode of a four-sector instrument. We also activated singly and doubly charged ions by low-energy collisions in an ion-trap mass spectrometer and investigated post source decompositions of matrix-assisted laser desorbed ions in a time-of-flight mass spectrometer. The various methods of extracting structural information give remarkably consistent results. The difference in the relative abundances of w_n and d_n ions of the singly charged oligonucleotides and the formation of $[a_3 - B_3]$ ions, where B_3 is the base on the third position, are effective for identification and distinction of pairs of isomeric tetranucleotides. A sufficient number of tetramers and pentamers were studied to enable us to propose a charge-remote mechanism for the formation of site-specific $[a_n - B_n]$ ion. (J Am Soc Mass Spectrom 1998, 9, 683–691) © 1998 American Society for Mass Spectrometry

The structure of DNA in living cells is constantly altered by endogenous chemical and enzymatic reactions and by exogenous chemical, physical, and biological agents. Fortunately, most enzymatically induced errors and structural alterations of DNA are repaired by the cell. If there is no repair, DNA synthesis past the damage site can lead to mutations (permanent alterations of the sequence of the DNA), which may lead to cancer or other disease state. Detection, identification, and quantification of mutations is important in understanding the mechanisms of mutagenesis and its role in various diseases, cancers, and aging. Because a wealth of structural information can be derived from mass spectrometry, we wish to develop it as an analytical tool for studying mutagenesis and for diagnosing disease.

Mutations have been studied in various ways, most of which have required screening and sequencing the DNA from progeny cell lines. Unfortunately, the DNA from progeny does not contain information that allows one to correlate damage with a particular mutation at a specific site. With the advent of methodology for producing oligonucleotides containing damage at a specific site, unraveling the precise structure-activity relationships in mutagenesis may be possible. To construct a statistically significant mutation spectrum, however, one generally acquires and sequences DNA from hundreds of progeny. The process of constructing a mutation spectrum would be greatly simplified if one could obtain the identity and frequency of individual mutations by a direct method such as mass spectrometry. As a starting point in the development of a mass spectrometric method, we chose small, T-rich oligonucleotides because T is an important target for DNA damage in at least one cancer (i.e., that of the skin) [1].

Skin cancer is among the most prevalent and will affect approximately one of four Americans. The UV portion of sunlight that penetrates the atmosphere produces *cis-syn* cyclobutane pyrimidine dimers and (6-4)-pyrimidine-pyrimidone photoproducts [1]. Although these photoproducts have been known for some time, only recently has it become possible to determine their mutagenic properties in vitro and in vivo [1]. In in vivo studies, bacteriophage or viral DNA containing an individual photoproduct at a unique site is introduced into living cells, and the progeny of the replicative

Address reprint requests to Michael L. Gross, Department of Chemistry, Washington University, Campus Box 1134, One Brookings Dr., St. Louis, MO 63130-4899. E-mail: mgross@wuchem.wustl.edu

1044-0305/98/$19.00
PII S1044-0305(98)00178-8

Received September 11, 1997
Revised January 7, 1998
Accepted January 13, 1998

bypass of the photoproduct are sequenced. Unfortunately, this method does not give direct information about the mutagenicity of the initial bypass event. For in vitro studies, the initial bypass products can be isolated, but because they occur in mixture, it has been difficult to determine the precise mutation spectrum by sequencing the bypass products alone. Rather than determine the precise mutation spectrum by cloning the bypass sequences and then sequencing DNA from hundreds of progeny, we suggest that an alternate and general methodology can be based on tandem mass spectrometry.

Briefly, the overall strategy that we propose is to use polymerase chain reaction (PCR) to amplify the bypass products attached to primers that contain appropriate restriction enzyme sites so that the PCR-amplified product can be restricted to give short oligonucleotides containing the sequence of interest. The mixture of short oligonucleotides would then be subjected to tandem mass spectrometry to identify and quantify the individual bypass products. In this article, we address the first step in achieving this goal; that is, to determine whether tandem masss spectrometry is sufficiently distinctive to characterize isomeric, T-rich oligomers. We chose T-rich tetramers and pentamers because T is the most susceptible of the nucleobases to UV damage.

Tandem mass spectrometry is an attractive approach to this sequencing problem owing to its high sensitivity and capability to provide primary-structure information. Early work on oligodeoxynucleotide sequencing was done with one stage of mass spectrometry after producing ions by using fast atom bombardment (FAB) or plasma desorption [2–6]. The largest oligodeoxynucleotide successfully sequenced by FAB coupled with one stage of mass spectrometry is a nucleotide decamer [7]. Cerny and co-workers [3] showed that the fragmentations of FAB-desorbed dinucleotides under the conditions of high-energy collisional activation are sequence specific for structural isomers. This approach was extended to small oligodeoxynucleotides (n = 3 to 6) [4].

Beauchamp and co-workers [8, 9] studied dinucleotides and determined the gas-phase acidities of four nucleic acid bases by using FAB-FT-ICR. McCloskey and co-workers [10] reported later that the fragmentations of the singly charged anions and cations of dinucleotides that occur in low-energy collision-activated dissociation (CAD) are similar to those initiated by high-energy collisions. Despite the early promise, FAB-MS/MS has not been used often for oligodeoxynucleotide sequencing owing to its relatively poor detection limit (approximately 10 nmol), especially for oligodeoxynucleotides with molecular weight larger than 1200, and to the wide range of molecular masses that must be detected when working with singly charged ions.

Electrospray ionization (ESI) offers higher sensitivity and better mass range than does FAB. McLafferty and co-workers [11, 12] successfully obtained sequence information for oligodeoxynucleotides ranging from 8- to 50-mers by dissociating the molecular ions with collisions in both the ESI source (ESI-source CAD) and in the cell of a Fourier transform (FT-ICR) mass spectrometer. Fragmentations of multiply charged oligodeoxynucleotide anions also occur after low-energy collisions, as was studied by McLuckey and co-workers [13–17], using the Paul ion trap, by Crain et al. [18] and by Gentil and Banoub [19], using a triple quadrupole instrument. Boschenok and Sheil [20] studied both low-energy and high-energy fragmentation pathways for ESI-produced small oligodeoxynucleotides (from 2- to 6-mers). Two isomeric oligodeoxynucleotide hexamers containing modified bases were also studied upon ESI introduction into an ion trap [21].

Significant progress has also been made on the application of matrix-assisted laser desorption ionization (MALDI)-TOF to oligodeoxynucleotides, which under post-source decomposition (PSD) conditions give information-rich, product-ion spectra. Oligodeoxynucleotides fragment much more readily than ribonucleotides under MALDI conditions [22, 23]. Buchanan and co-workers [24–27] demonstrated successful structural characterization of small native and modified oligodeoxynucleotides by using UV-MALDI FTMS.

Although many others have studied the fragmentations of singly and multiply charged oligodeoxynucleotides, comparisons of fragmentations of ions produced by different ionization methods (ESI vs. MALDI) or activated by different processes (low-energy CAD vs. high-energy CAD) have yet to be made. In this article, we compare four methods of activation of four pairs of isomeric T-rich tetramers and three isomeric pentamers not only to determine whether one can distinguish structural isomers but also to understand the mechanisms that govern the fragmentations.

Experimental

Materials

All deoxyoligonucleotide samples used in this study were synthesized (on the 1 μmol scale) by the Nucleic Acid Chemistry Laboratory at Washington University (St. Louis, MO) and were used without further purification. All samples were obtained as either the sodium salt or the free acid.

Electrospray Mass Spectrometry on a Four-Sector Instrument

ESI experiments were carried out on a VG ZAB-T four-sector tandem mass spectrometer [28] coupled with a VG Analytical ESI source (Manchester, UK). Mass spectrometry data were obtained by scanning MS1 at a mass resolving power of approximately 1500. Tandem mass spectra were acquired after activating the ion of interest by collisions with helium gas and ana-

lyzing the fragment masses with the second double-focusing mass spectrometer. Data were acquired and recorded with the manufacturer's DEC Alpha 3000 workstation equipped with OPUS V 3.2X data system and interfaced to the mass spectrometer via a VG SIOS I unit.

Oligodeoxynucleotides were dissolved in a solution of 1% TFA in 50/50 methanol/water. Acidic conditions were used to minimize multiple charging. The same solvent solution was used as the mobile phase and was delivered by an infusion syringe pump (Harvard Apparatus, South Natick, MA) at a flow rate of 10 μL/min. The sample (in 20 μL) was injected through a Rheodyne 7125 loop injector (Cotati, CA). Nitrogen was used as a bath and nebulizer gas with flow rates of 300 and 12 L/h, respectively, to provide coaxial flow of warm (~80 °C) bath gas, which aided the desolvation process. Ion-spray needle voltages were from 7.8 to 8.5 kV. Singly charged anions were accelerated to 4 kV and detected with a single-point detector to obtain mass spectra. The first-stage spectrometer was scanned at a rate of 15 s/decade over the mass range of m/z 150 to 1500 with a 1 s delay between scans. ESI-source CAD were induced by increasing the sampling cone voltage from 4.1 to 4.4 kV.

The tandem mass spectra of ESI-produced ions were recorded by focusing with MS1 the parent-ion beam into the collision cell, reducing the parent-ion beam intensity by 80% by adding sufficient helium gas, and scanning MS2. Because collisional activation of multiple-charged ions produces fragment ions with a mass-to-charge ratio value higher than the parent ion and the software did not allow a scan beyond the mass-to-charge ratio of the parent ion, collisional activation experiments were carried out only with singly charged ions.

Electrospray Mass Spectrometry on an Ion Trap Instrument

ESI experiments were also performed on a Finnigan LCQ instrument. Oligodeoxynucleotides were dissolved in a solution of 1% NH_4OH in 50/50 methanol/water to give a concentration of 10 pmol/μL; basic conditions were used to produce singly and doubly charged anions. The same solvent solution was used as the carrier solvent for electrospray. The flow rate was 5 μL/min. The spray voltage was kept at 4.6 kV, the capillary temperature was set to 200 °C, and the capillary voltage was adjusted to −13.0 V for negative-ion detection. The instrument was operated at a background pressure of 2×10^{-5} torr, as measured by an ion gauge. In all experiments, helium was introduced to an estimated pressure of 1 mtorr for improving the trapping efficiency. The background helium gas also served as collision gas during the CAD event. The collision energy was 40% and 20% of the maximum available from a 5-V tickle voltage for singly and doubly charged anions, respectively, and the scan rate for product ions was 5000 u/s. Data were collected and analyzed with both the instrument software and the ICIS software developed by the manufacturer.

MALDI-PSD Experiments

MALDI-PSD was carried out on a PerSeptive Biosystems Voyager RP MALDI-TOF instrument. A saturated solution of 4-hydroxy-3-methoxy cinnamic acid in 50% 0.1 M ammonium citrate and 50% CH_3CN containing 1% TFA was used as matrix. Cation-exchange resin beads, in the NH_4^+ form, were used to minimize the contamination of alkali-metal ions. Samples (in 1 μL) were premixed with the matrix solution (1 μL) before they were loaded onto the sample plate. A new portion of the sample was used each time to reduce the contamination due to repeated sample handling. Negative ions were desorbed with a nitrogen laser (337 nm) and accelerated with a potential of 25 kV. PSD was induced by increasing the laser power. The singly charged molecular ion (mass width of ±7 u) was chosen as the precursor ion for the PSD experiments.

Results and Discussion

CAD of Tetradeoxynucleotides

We prepared singly charged $[M - H]^-$ ions of tetradeoxynucleotides by using electrospray and MALDI and activated the electrospray-generated ions in the ion source of a four-sector mass spectrometer (ESI-source CAD) and by high-energy collisions after a first stage of mass analysis. We also used ESI to produce, in an ion-trap mass spectrometer, multiply charged, closed-shell anions, which we activated by low-energy collisions. The doubly charged ions are produced at comparable abundance as the singly charged species. To complete the comparison, we generated $[M - H]^-$ anions by MALDI and monitored their PSD in a reflectron TOF mass spectrometer. The nomenclature for assigning the product ions is by McLuckey and Habibi-Goudarzi [17].

We chose as a first step in the evaluation of methods the characterization of 5′-dTpdApdTpdT-3′ or more simply d(TATT). We begin with ESI-source CAD because it is the simplest and the most readily implemented method of activation, and no tandem mass spectrometer is required. ESI-source CAD can also allow reasonable mass resolving power of the product-ion spectrum. We cannot distinguish the product ions d_3/w_3 at m/z 938 and b_3/y_3 at m/z 858 (see Figure 1A) because the d(TATT) begins and ends with T. Two potentially useful product ions for distinguishing isomers are the w_2 ion of m/z 625 and the $[a_3 - B_3$ (Thy)] of m/z 714. Although Boschenok and Sheil [20] observed no significant enhancement of sequence-specific product ions at higher skimmer potential, we did see increased fragmentation owing to the greater collision energy at the higher potential. ESI-source CAD is

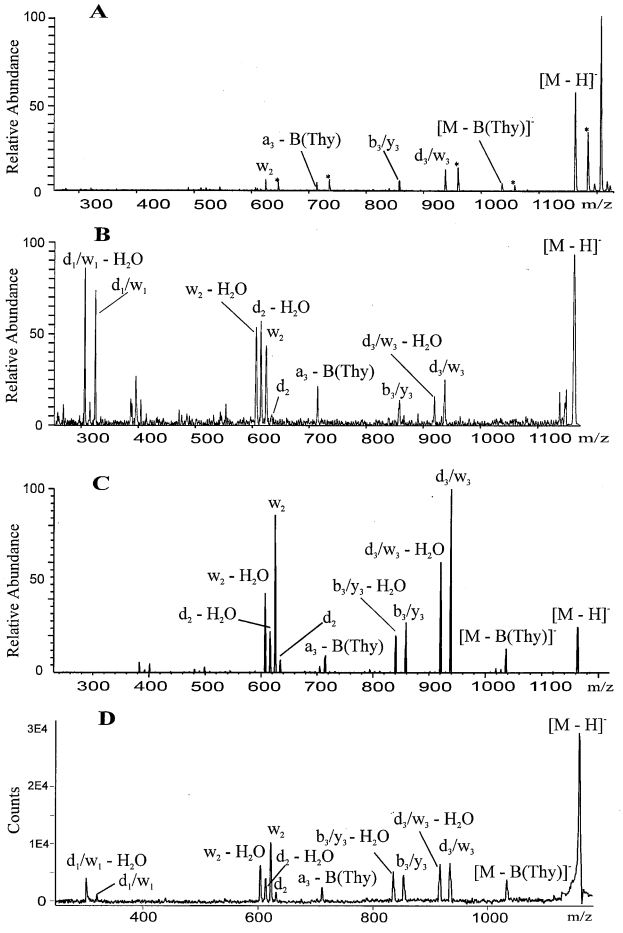

Figure 1. CAD spectra of the $[M - H]^-$ ions of d(TATT): (**A**) ESI-source CAD spectrum (10 pmol/μL), (**B**) High-energy CAD product-ion spectrum of ESI-produced ions (30 pmol/μL), (**C**) Low-energy product-ion spectrum from the ion trap (10 pmol/μL), (**D**) MALDI-PSD spectrum (5 pmol/μL).

a useful indicator of the fragmentation chemistry of these pure compounds, but it is not a general method to determine a compound in a mixture.

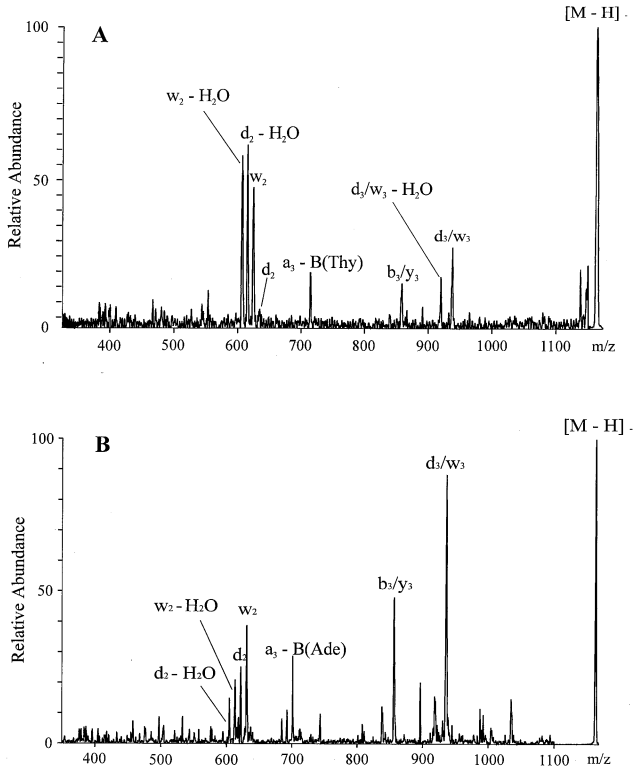

Figure 2. Comparison of high-energy product-ion spectra of ESI-produced ions for the structural isomers: (**A**) d(TATT) and (**B**) d(TTAT).

An unambiguous means of obtaining the product-ion spectrum is with the four-sector instrument. The high-energy (HE) CA of ESI-produced ions yields more fragment ions and more structural information (see Figure 1B), but the method is not highly efficient (the magnification factor is 200 for the product-ion region of the spectrum in Figure 1B). Unlike the product-ion spectra of ions produced by MALDI or in the ion trap, we see in the HE CAD spectrum the full complement of w_n/d_n ions and the interesting $[a_3 - B_3 (Thy)]$ ion.

Table 1. Comparison product-ion spectra of d(TATT) and d(TTAT) taken with four different tandem mass spectrometry methods

	d(TATT)						d(TTAT)					
			Low-energy CAD RA(%)						Low-energy CAD RA(%)			
m/z	Ion type	High-energy CAD RA(%)	$[M - H]^-$	$[M - 2H]^{2-}$	Source CAD RA(%)	MALDI-PSD RA(%)	Ion type	High-energy CAD RA(%)	$[M - H]^-$	$[M - 2H]^{2-}$	Source CAD RA(%)	MALDI-PSD RA(%)
938	d_3/w_3	28	100	100	100	67	d_3/w_3	92	100	67	40	47
858	b_3/y_3	17	30	18	40	47	b_3/y_3	53	28	9	60	30
706		ND[a]	ND	ND	ND	ND	$a_3 - A$	31	90	100	100	55
714	$a_3 - T$	20	10	25	25	27		ND	ND	ND	ND	ND
634	d_2	<5	8	ND	ND	20	w_2	41	65	18	87	100
625	w_2	48	90	40	30	100	d_2	25	5	ND	11	19
616	$d_2 - H_2O$	64	24	ND	ND	41	$w_2 - H_2O$	20	43	ND	64	62
607	$w_2 - H_2O$	58	44	ND	<5	64	$d_2 - H_2O$	15	15	2	26	34
321	d_1/w_1	ND	NA[b]	8	<5	NA	d_1/w_1	ND	NA	64	35	NA

[a]ND = not detected.
[b]NA = not available.

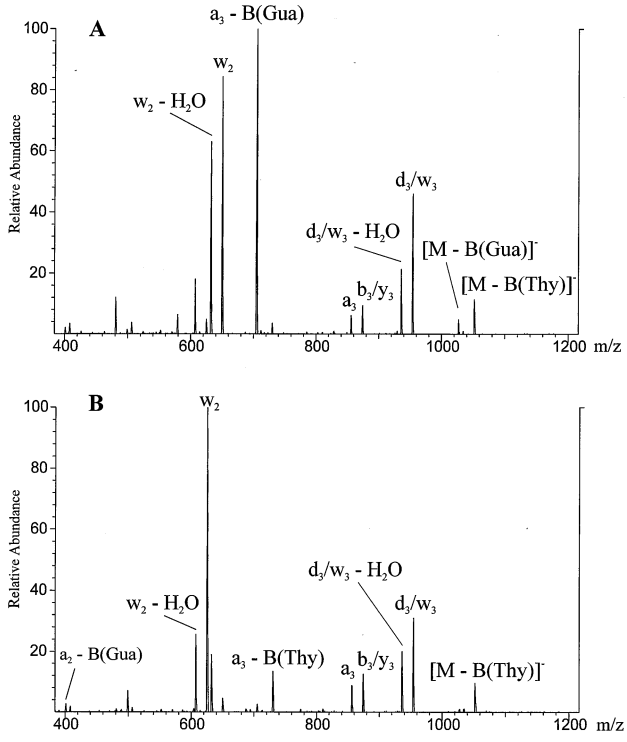

Figure 3. Comparison of low-energy product-ion spectra from the ion trap for the singly charged structural isomers: (**A**) d(TTGT) and (**B**) d(TGTT).

The low-energy CAD spectrum of the $[M - H]^-$ is similar to that of ions formed at high-collision energy except the low-mass product ions are missing owing to the low-mass cutoff of the ion trap mass spectrometer (Figure 1C). The efficiency of the method is significantly better than high-energy CAD because the precursor ion is submitted to many low-energy collisions, and the yield for ion collection is high.

The PSD of MALDI-produced ions give a product-ion spectrum that is similar to the above three spectra (see Figure 1D). Once again we see the $[a_3 - B_3$ (Thy)] ion and a set of w_n/d_n ions, which appear to favor the w series as Hettich, Buchanan, and co-workers reported [24–27]. MALDI is competitive in sensitivity with the ion trap, but it suffers from the poorest resolving power, at least with our TOF mass spectrometer, which did not have the capability for delayed extraction at the time of this study.

In the next few sections, we compare and contrast the fragmentation chemistry of four isomeric pairs of tetradeoxynucleotides. We chose the structural isomers because they are difficult to distinguish by classic biological techniques, and they set the stage for studies of larger oligodeoxynucleotides that are rich in T. Furthermore, they are a challenge for mass spectrometric methods because the subject molecules begin and end with T. For brevity sake, but without sacrificing detail, we identify for each isomeric pair the distinctive product ions and emphasize a different method of producing and observing the product ions.

d(TATT) and d(TTAT). For this pair, we emphasize high-energy CAD. The important ions for distinguishing isomers are $[a_3 - B_3]$ ions and w_2/d_2 ions, where w_2 ions are probably the more important contributor to the peak (Figure 2). To confirm sequence, the w_1 and w_3 ions are also important. For d(TATT), Thy is the base lost, whereas for d(TTAT), Ade is lost, giving a clean and simple distinction of the two isomers. Note there is no $[a_2 - B_2]$ ion.

The ESI-source CAD, low-energy CAD of singly and doubly charged precursor ions, and the PSD spectra of MALDI-produced ions contain the same information as the high-energy CAD spectra (see Table 1). Any one of the four methods can be effectively used to distinguish the isomeric pair.

d(TGTT) and d(TTGT). For this pair, we emphasize low-energy CAD spectra (Figure 3) that were obtained with the ion-trap mass spectrometer although the same

Table 2. Comparison product-ion spectra of d(TTGT) and d(TGTT) taken with four different tandem mass spectrometry methods

	d(TTGT)						d(TGTT)					
			Low-energy CAD RA(%)						Low-energy CAD RA(%)			
m/z	Ion type	High-energy CAD RA(%)	$[M - H]^-$	$[M - 2H]^{2-}$	Source CAD RA(%)	MALDI-PSD RA(%)	Ion type	High-energy CAD RA(%)	$[M - H]^-$	$[M - 2H]^{2-}$	Source CAD RA(%)	MALDI-PSD RA(%)
954	d_3/w_3	100	54	100	52	19	d_3/w_3	100	30	100	35	51
874	b_3/y_3	26	10	56	100	13	b_3/y_3	22	16	74	70	43
730		ND[a]	ND	ND	ND	ND	$a_3 - A$	ND	17	56	25	25
705	$a_3 - G$	45	100	24	18	58		ND	ND	ND	ND	ND
650	w_2	20	84	36	100	100	d_2	7	<5	ND	15	18
632	$w_2 - H_2O$	70	64	<5	53	72	$d_2 - H_2O$	15	16	ND	35	37
625	d_2	25	<5	ND	<5	22	w_2	25	100	55	45	100
607	$d_2 - H_2O$	53	18	ND	13	34	$w_2 - H_2O$	22	24	<5	20	49
321	d_1/w_1	ND	NA[b]	ND	100	NA	d_1/w_1	ND	NA	ND	100	NA

[a]ND = not detected.
[b]NA = not available.

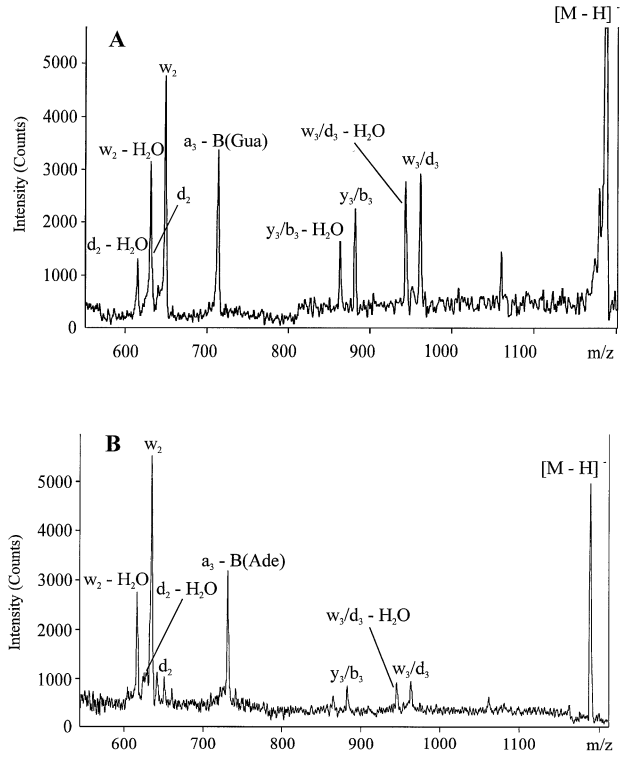

Figure 4. Comparison of MALDI-PSD spectra for the structural isomers: (**A**) d(TAGT) and (**B**) d(TGAT).

qualitative information is in the other three pair of product-ion spectra (Table 2). The singly charged molecular anions give w_3/d_3 at m/z 954 and b_3/y_3 at m/z 874. Although it is likely that the ions are w_3, and not d_3, there is no ambiguity for the w_2 ions; for d(TGTT), w_2 and d_2 are of m/z 625 and 650, respectively. For d(TTGT), on the other hand, the mass-to-charge ratio assignments are reversed. As before, the w ions are more abundant than the d ions and the w_2 and d_2 ions are accompanied by fragment ions that are 18 u lower, presumably from water loss from a deoxyribose. We also note that the distinction of isomers afforded by the $[a_3 - B_3]$ ions is facile and that the relative abundances of $[a_2 - B_2]$ ions are <5%. This latter observation has important mechanistic implications.

Turning to doubly charged ions, we see identical qualitative information in the low-energy product-ion spectrum, but the fragmentation can be induced at lower collision energy presumably owing to the increased coulombic repulsion in the doubly charged ions. One also finds doubly charged product ions in the low-energy spectrum of $[M - 2H]^{2-}$.

d(TAGT) and d(TGAT). For this pair of isomers, we emphasize the PSD of MALDI-produced $[M - H]^-$ ions. The trend established for the two previously discussed pairs of isomeric tetradeoxynucleotides [i.e., that the isomers are readily distinguished on the basis of the w_2 and $[a_3 - B_3]$ ions (Figure 4)] is maintained. For d(TAGT), w_2 is of m/z 650, and only a trace of d_2 ions forms as indicated by a peak shoulder. Whereas for d(TGAT), the w_2 ion is of m/z 634, and the d_2 ion at m/z 650 is of low abundance. The $[a_3 - B_3]$ ions are readily apparent: for d(TAGT), the base that is lost is Gua, whereas for d(TGAT), it is Ade. These qualitative ion-chemistry patterns are shared by the precursor ions undergoing ESI-source, high-energy, low-energy, and PSD (Table 3).

d(TACT) and d(TCAT). The results for the last pair of isomeric tetradeoxynucleotides, which we investigated, leaves little doubt that isomers of this class are distinguishable by tandem mass spectrometry of negative ions. For d(TACT), the mass-to-charge ratio values and the relative abundances are simply reversed. Both isomers also give the expected and distinctive $[a_3 - B_3]$ ions. The isomeric-specific patterns can be recognized in product-ion spectra from the other three methods (Table 4).

Table 3. Comparison product-ion spectra of d(TAGT) and d(TGAT) taken with four different tandem mass spectrometry methods

	d(TAGT)						d(TGAT)					
			Low-energy CAD RA(%)						Low-energy CAD RA(%)			
m/z	Ion type	High-energy CAD RA(%)	$[M - H]^-$	$[M - 2H]^{2-}$	Source CAD RA(%)	MALDI-PSD RA(%)	Ion type	High-energy CAD RA(%)	$[M - H]^-$	$[M - 2H]^{2-}$	Source CAD RA(%)	MALDI-PSD RA(%)
963	d_3/w_3	100	57	100	100	61	d_3/w_3	30	40	42	100	17
883	b_3/y_3	43	10	43	82	48	b_3/y_3	21	7	29	52	15
730		ND[a]	ND	ND	ND	ND	$a_3 - A$	32	100	100	78	57
714	$a_3 - G$	16	81	26	62	70		ND	ND	ND	ND	ND
605	w_2	53	100	32	80	100	d_2	12	<5	ND	<5	18
634	d_2	8	<5	ND	<5	<5	w_2	100	56	19	73	100
632	$w_2 - H_2O$	26	35	<5	20	66	$d_2 - H_2O$	<5	8	<5	15	<5
616	$d_2 - H_2O$	7	10	ND	30	27	$w_2 - H_2O$	72	16	ND	10	49
321	d_1/w_1	ND	NA[b]	ND	34	NA	d_1/w_1	ND	NA	ND	30	NA

[a]ND = not detected.
[b]NA = not available.

Table 4. Comparison product-ion spectra of d(TACT) and d(TCAT) taken with four different tandem mass spectrometry methods

	d(TACT)						d(TCAT)					
			Low-energy CAD RA(%)						Low-energy CAD RA(%)			
m/z	Ion type	High-energy CAD RA(%)	$[M-H]^-$	$[M-2H]^{2-}$	Source CAD RA(%)	MALDI-PSD RA(%)	Ion type	High-energy CAD RA(%)	$[M-H]^-$	$[M-2H]^{2-}$	Source CAD RA(%)	MALDI-PSD RA(%)
923	d_3/w_3	95	59	100	51	ND	d_3/w_3	100	66	66	73	18
843	b_3/y_3	35	12	7	90	ND	b_3/y_3	10	11	9	100	<5
714	$a_3 - C$	38	100	4	12	91		ND[1]	ND	ND	ND	ND
690		ND[a]	ND	ND	ND	ND	$a_3 - A$	23	67	100	25	80
634	d_2	<10	<5	ND	12	19	w_2	100	100	8	97	100
616	$d_2 - H_2O$	20	7	ND	ND	35	$w_2 - H_2O$	30	29	ND	42	37
592	w_2	100	63	21	68	100	d_2	20	ND	ND	ND	<5
610	$w_2 - H_2O$	33	22	ND	20	61	$d_2 - H_2O$	18	12	2	10	32
321	d_1/w_1	ND	NA[b]	2	100	NA	d_1/w_1	ND	NA	63	100	NA

[a]ND = not detected.
[b]NA = not available.

d(TGTTT), d(TTGTT), and d(TTTGT). To establish that the absence of $[a_2 - B_2]$ ions pertains to pentamers, we studied three isomeric T-rich isomers. We chose Gua as the other base because it is the most readily lost and is the best test for site specificity. For singly and doubly charged precursor ions, the fragments $[a_3 - B_3]$ and $[a_4 - B_4]$ ions are always formed. All the spectra of tetramers and pentamers show that the loss of neutral base Gua from the a_3 ion is the most facile, whereas the loss of neutral base Thy is the least, and the loss of neutral base Ade and Cyt are intermediate. The $[a_2 - B_2]$ ion is not observed except for d(TGTTT) where the highly favored loss of Gua occurs to give this ion at low abundance (see Figure 5).

Mechanisms of CAD of the Oligodeoxynucleotide Anions

The reactions occurring upon high-energy collisional activation of singly charged and low-energy collision activation of the doubly charged tetranucleotide anions give rise to very abundant w-series ions and an $[a_3 - B_3]$ ion. Certain factors pertaining to the $[a_3 - B_3]$ ion formation bear on mechanism, and they are summarized here. The obvious precursors for the $[a_3 - B_3]$ ions, besides the $[M - H]^-$, are a_3 and $[M - H - B]^-$, but these latter two ions are of low abundances or sometimes not seen in the CAD spectra of the tetradeoxynucleotides. These observations indicate that the formation of the $[a_3 - B_3]$ ion either involves a short-lived intermediate whose lifetime is shorter than the time scale of the mass-spectrometry measurement or it is a concerted process. Furthermore, there is a strong, nearly overwhelming preference for forming the $[a_3 - B_3]$ ion rather than the $[a_2 - B_2]$ ion. The only tetranucleotide that exhibits a small abundance of $[a_2 - B_2]$ is d(TGTT) (Figure 3) because the elimination of Gua is most favored, Thy least favored, and Cyt and Ade are intermediate. This order is parallel to that of the gas-phase proton affinities of the nucleobases [29]. To provide further evidence that there is positional selectivity in addition to base dependence governing the formation of $[a_3 - B_3]$ ion, we investigated the fragmentations of the three isomeric 5-mers. Low-energy collision conditions (see Figure 5) favor loss of neutral Gua over that of Thy from both a_3 and a_4 ions. The $[a_2 - B_2]$ ions is not detectable, except when Gua is at the

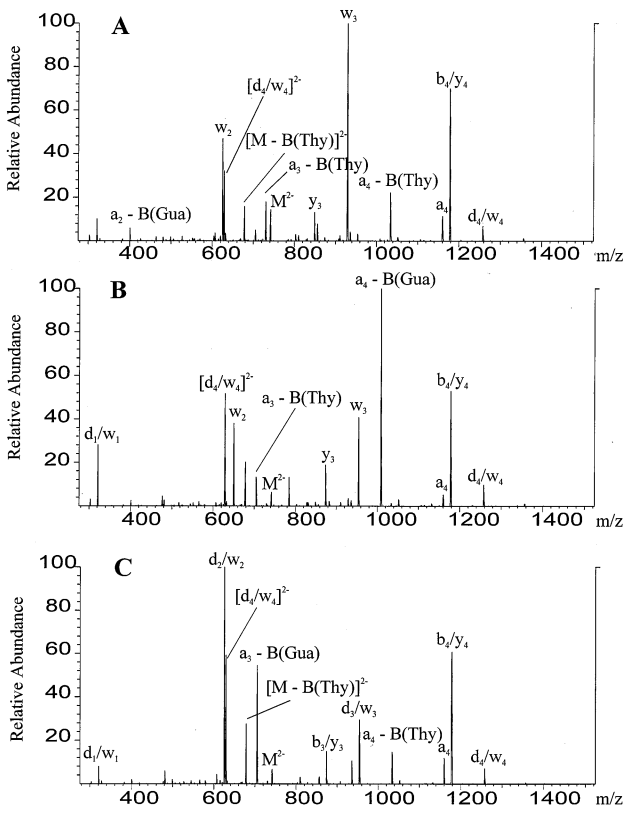

Figure 5. Comparison of low-energy product-ion spectra from the ion trap for the doubly charged structural isomers: (**A**) d(TGTTT), (**B**) d(TTTGT), (**C**) d(TTGTT).

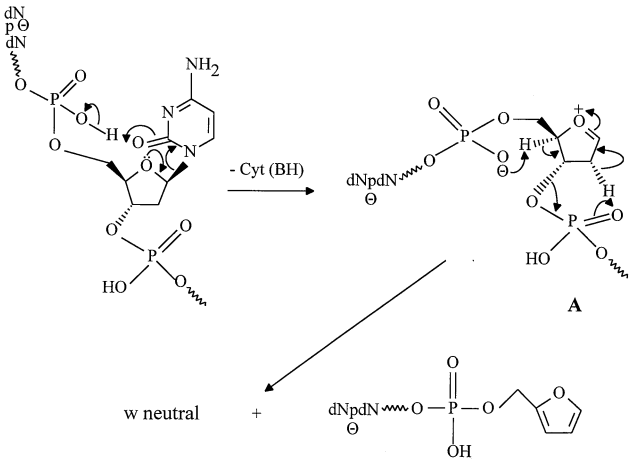

Scheme I

2-position, confirming that positional selectivity plays a role in the formation of $[a_3 - B_3]$ and $[a_4 - B_4]$ ions.

The formation of w and $[a_n - B_n]$ ions from singly charged precursors has been studied by us [3, 4] and many others [8, 9, 10, 30–33]. The mechanism involving multiply charged precursors has also been investigated by many groups [11–17, 34]. Most proposed two-step 1,2-elimination processes that account for the formation of $[a_n - B_n]$ ions and the complementary w series ions. The two-step 1,2-elimination mechanism, however, *cannot* explain the site-specific base loss or the absence of intermediates. Therefore, we propose an alternate charge-remote mechanisms for $[a_n - B_n]$, and this is illustrated for loss of cytosine in Scheme I, for singly charged precursor ions. Protonation of the nucleobase initiates the neutral base loss and thereby leads to the backbone cleavage to form the $[a_n - B_n]$ ion and w neutral. The preference for losing G > A, C > T follows the order of proton affinities of the nucleobases [29], which is consistent with the first step being proton transfer from the acidic P–OH. We note here that the intermediate A is zwitterionic and would be expected to be short-lived, explaining why no intermediates were usually observed on the time scale of mass spectrometry analysis. The nearby acidic hydrogen on the 5′ phosphate is critical because it is transferred in the first step. Without this hydrogen, the base cannot be easily protonated and the $[a_n - B_n]$ ion cannot form. Although w-series ions are complementary to $[a - B]$ ions, there may be other mechanisms for producing w ions (e.g., a 1,2-elimination), explaining why w ions are often more abundant than $[a - B]$ ions from doubly charged precursors.

Working with this assumption, we considered the charge-remote fragmentation of the three most likely charge isomers of tetramer $[M - H]^-$ ions. When the negative charge is on the first phosphate from the 5′ end (see Scheme IIA), the availability of an acidic hydrogen on the second phosphate enables the formation of $a_3 - B_3$. When the negative charge is on the second phosphate (see Scheme IIB), the acidic hydrogen of the first phosphate from the 5′ end is available to protonate $base_2$, but the $[a_2 - B_2]$ species is neutral and will not be detected. The complementary fragment will carry the charge and be detected as a w_2 ion. Using the same

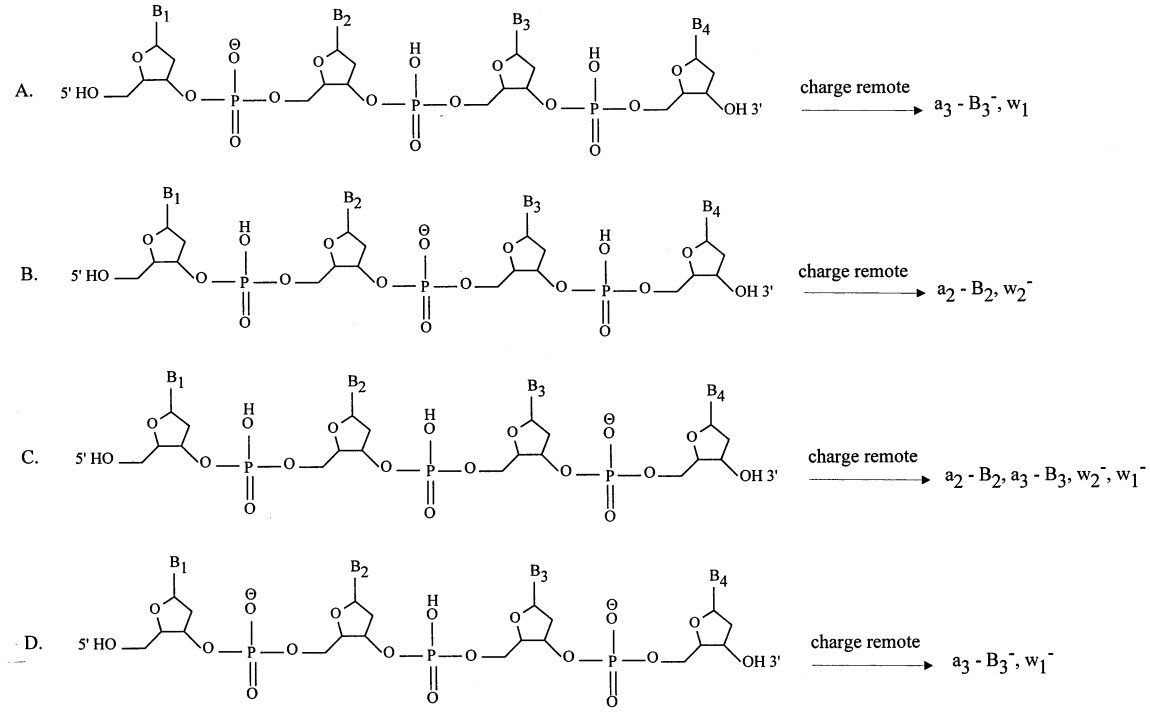

Scheme II

analysis, we reason that $[a_2 - B_2]$ neutral, $[a_3 - B_3]$ neutral, w_1 and w_2 ions will form when the charge is on the third phosphate (see Scheme IIC). The same analysis on the most probable doubly charged precursor ions (Scheme IID) shows, again, only $[a_3 - B_3]$ ion can form. This explains the site specificity of the base loss.

Conclusions

Results of ESI-source CAD, low-energy CAD by LCQ, high-energy ESI-MS/MS and MALDI-PSD experiments show that mass spectrometry generates sufficient fragment ions for distinguishing structural isomers for small oligodeoxynucleotides. These different methods of activation give similar fragmentation patterns, indicating that the chemistry governing the fragmentation is also similar.

On the basis of the results from a substantial series of tetramers and pentamers, we propose a new charge-remote mechanism involving protein transfer from the adjoining phosphate for the formation of $[a_n - B_n]$. We are conducting two sequel studies. The first tests the applicability of the mechanism and ability to distinguish isomers to 6-, 8-, and 10-mers that are rich in T. The second has an analytical focus and will evaluate the capabilities of mass spectrometric methods to analyze mixtures of isomeric oligonucleotides.

Acknowledgment

This work was supported by the National Institutes of Health, National Center for Research Resources (grant no. 2P41RR00954) and by NIH grant no. P01CA49210.

References

1. Taylor, J.-S. *Acc. Chem. Res.* **1994,** *27*, 76.
2. Budzikiewicz, H. *Mass Spectrom. Rev.* **1985,** *4*, 145.
3. Cerny, R. L.; Gross, M. L.; Grotjahn, L. *Anal. Biochem.* **1986,** *156*, 424.
4. Cerny, R. L.; Tomer, K. B.; Gross, M. L.; Grotjahn, L. *Anal. Biochem.* **1987,** *165*, 175.
5. McNeal, C. J.; Narang, S. A.; McFarlane, R. D.; Hsiung, H. M.; Brousseau, K. R. *Proc. Natl. Acad. Sci.* **1980,** *77*, 735.
6. McNeal, C. J. *Nucl. Instrum. Methods* **1982,** *198*, 139.
7. Grotjahn, L.; Frank, R.; Blocker, H. *Nucleic Acids Res.* **1982,** *10*, 4671.
8. Rodgers, M. T.; Campbell, S.; Marzluff, E. M.; Beauchamp, J. L. *Int. J. Mass Spectrom. Ion Processes* **1994,** *137*, 121.
9. Rodgers, M. T.; Campbell, S.; Marzluff, E. M.; Beauchamp, J. L. *Int. J. Mass Spectrom. Ion Processes* **1995,** *148*, 1.
10. Phillips, D. R.; McCloskey, J. A. *Int. J. Mass Spectrom. Ion Processes* **1993,** *128*, 61.
11. Little, D. P.; McLafferty, F. W. *J. Am. Chem. Soc.* **1995,** *117*, 6783.
12. Little, D. P.; Chorush, R. A.; Speir, J. P.; Senko, M. W.; Kelleher, N. L.; McLafferty, F. W. *J. Am. Chem. Soc.* **1994,** *116*, 4893.
13. McLuckey, S. A.; Van Berkel, G. J.; Gilsh, G. L. *J. Am. Soc. Mass Spectrom.* **1992,** *3*, 60.
14. McLuckey, S. A.; Habibi-Goudarzi, S. *J. Am. Soc. Mass Spectrom.* **1994,** *5*, 740.
15. Habibi-Goudarzi, S.; McLuckey, S. A. *J. Am. Soc. Mass Spectrom.* **1995,** *6*, 102.
16. McLuckey, S. A.; Vaidyanathan, G.; Habibi-Goudarzi, S. *J. Mass Spectrom.* **1995,** *30*, 1222.
17. McLuckey, S. A.; Habibi-Goudarzi, S. *J. Am. Chem. Soc.* **1993,** *115*, 12085.
18. Crain, P. F.; Gregson, J. M.; McCloskey, J. A.; Nelson, C. C.; Peltier, J. M.; Phillips, D. R.; Pomerantz, S. C.; Reddy, D. M. In *Mass Spectrometry in the Biological Sciences*; Burlingham, A. L.; Carr, S. A., Eds.; Humana Press: Totowa, NJ, 1996; p 497.
19. Gentil, E.; Banoub, J. *J. Mass Spectrom.* **1996,** *31*, 83.
20. Boschenok, J.; Sheil, M. M. *Rapid Commun. Mass Spectrom.* **1996,** *10*, 144.
21. McLuckey, S. A.; Habibi-Goudarzi, S. *J. Am. Soc. Mass. Spectrom.* **1994,** *5*, 740.
22. Kirpekar, F.; Nordhoff, E.; Kristiansen, K.; Roepstorff, P.; Lezius, A.; Hahner, S.; Karas, M.; Hillenkamp, R. *Nucleic Acids Res.* **1994,** *22*, 3866.
23. Nordhoff, E.; Kirpekar, F.; Karas, M.; Cramer, R.; Hahner, S.; Hillenhamp, F.; Kristiansen, K.; Roepstorff, P.; Lezius, A. *Nucleic Acids Res.* **1994,** *22*, 2460.
24. Hettich, R. L.; Buchanan, M. V. *J. Am. Soc. Mass Spectrom.* **1991,** *2*, 402.
25. Hettich, R. L.; Buchanan, M. V. *Int. J. Mass Spectrom. Ion Processes* **1991,** *111*, 365.
26. Stemmler, E. A.; Buchanan, M. V.; Hurst, G. B.; Hettich, R. L. *Anal. Chem.* **1995,** *67*, 2924.
27. Stemmler, E. A.; Buchanan, M. V.; Hurst, G. B.; Hettich, R. L. *Anal. Chem.* **1994,** *66*, 1274.
28. Gross, M. L. *Methods in Enzymology, Vol. 193, Mass Spectrometry*; McCloskey, J. A., Ed.; Academic: San Diego, 1990; pp 131–153.
29. Greco, F.; Lugiori, A.; Sidona, G.; Uccella, N. *J. Am. Chem. Soc.* **1990,** *112*, 9092.
30. Nordhoff, E.; Karas, M.; Cramer, R.; Hahner, S.; Hillenhamp, F.; Kirpekar, F.; Lezius, A.; Muth, J.; Meier C.; Engels, J. W. *Nucleic Acids Res.* **1995,** *30*, 99.
31. Zhu, L.; Parr, G. R.; Fitzgerald, M. C.; Nelson, C. M.; Smith, L. M. *J. Am. Chem. Soc.* **1995,** *117*, 6048.
32. Kirpekar, F.; Nordhoff, E.; Kirstiansen, K.; Roepstorff, P.; Lezius, A.; Hahner, S.; Hillenkamp, F. *Rapid Commun. Mass Spectrom.* **1995,** *9*, 525.
33. Hettich, R. L.; Stemmler, E. A. *Rapid Commun. Mass Spectrom.* **1996,** *10*, 321.
34. Barry, J. P.; Vouros, P.; Schepdael, A. V.; Law, S. J. *J. Mass Spectrom.* **1995,** *30*, 993.